Journal of Engineering Research

Volume 3
Issue 4 *(December)*

Article 2

2019

The Lateral Distortional Buckling of I-Plate Girders

Hanan Gamal, M. El-Boghdadi, M. F. Hassanein, A. M. EL Hadidy

The Lateral Distortional Buckling of I-Plate Girders

Hanan Gamal, M. El-Boghdadi, M. F. Hassanein and A. M. EL Hadidy

***Abstract*-This paper presents a numerical study for lateral distortional buckling of I-plate girders (LDBIPGs) by using the general-purpose finite element package ABAQUS (version 6.13) software. 3-D finite element (FE) models for simply supported IPGs subjected to two cases of loading are built. The first case of loading was uniform end moment that was introduced by a couple of forces applied at the top and bottom flanges of the IPGs. The second case of loading was a concentrated load at the shear center in the mid-span. First, shell finite element models are validated by comparing the FE critical bending moment ($M_{cr,FE}$) by the critical bending moment in EC3 code ($M_{cr,o,LTB}$). The results indicate that the $M_{cr,FE}$ was in good agreement with $M_{cr,o,LTB}$. Secondly, a preliminary analysis is conducted to the relative girder slenderness (λ) where the LDB too place. Finally, a parametric study is carried out on simply supported IPGs regarding to the span length, the flange cross-section dimensions and the thickness of the web. The results showed that increasing the length of girders decreases $M_{cr.FE}$ and increase in the bending coefficient factor (C_b). Also, decreasing in the web plate slenderness ratio (h_w/t_w) works on increasing in $M_{cr.FE}$ values and C_b. The results also showed that the increasing in the thickness of flange increases $M_{cr.FE}$ and increase the value of C_b with small value. As a result of parametric study, the mean value and standard deviation of C_b for LDB mode are 1.16 and 0.08 respectively for λ limits (90:130). For λ limits (131:175), the mean value and standard deviation of C_b are 1.27 and 0.03 respectively. As for λ limits (176:221), the mean value and standard deviation of C_b are 1.32 and 0.02 respectively.**

Keywords: Lateral distortional buckling – uniform end moment – bending coefficient factor.

1. INTRODUCTION

It is well known that I-steel plate girders (IPGs), obtained by web plate elements and flanges, when these girders are loaded in its principle plane, it may occur buckling out of plane if it does not have sufficient lateral stiffness [1-6]. These girders can buckle by lateral deflection and twisting of the cross-section. This phenomenon called by lateral torsional buckling (LTB) and this type of buckling involve lateral deflection and twist in upper flange liked in the lower flange as shown in Fig. 1-a. There is another type of buckling is known as local buckling (LB) in which compression elements (compression flanges or webs) can buckle locally over a short length of the member with local changes in the shape of cross section as shown in Fig. 1-b. It is important to know that two modes of buckling (lateral torsional buckling and local buckling) may interact to consist anther mode of buckling called by lateral distortional buckling (LDB) as can be seen in Fig. 1-c.

In intermediate-length IPGs with slender webs and stocky flanges the overall lateral deformation of the IPGs may be accompanied by web distortions [7-10]. This mode of buckling also placed on IPGs, which have a large flexural rigidity in their loaded plane and a small flexural rigidity in the other plane. In this mode, the flange can deflect laterally with rotation in upper flange non-in the lower flange and the web will be distorted. This buckling mode reduced torsional rigidity of the section and this obvious in plate girders with slender and un-stiffened webs than in stocky webs [9-11].

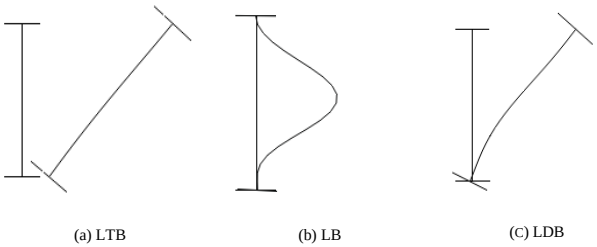

Fig.1. Different buckling modes of steel IPGs.

Many studies have been performed separately on LB and LTB, and codes of practice for the design of structural steelwork contain the relevant clauses. LDB is less well known and has long been ignored in design specification [10, 11]. Work in the last years has added much to our understanding of this type of buckling and after many years of relative neglect, LDB has recently been the subject of a good deal [10-13].

The research conducted herein on the behavior of the IPGs were developed using the general-purpose FE package ABAQUS [14] based upon the availability of trusted FE models in the literature.

In 2013, Hassanein and Silvestre investigated stainless steel IPGs numerically [15]. Moreover, the flexural strength of hollow tubular flange plate girder was studied by Hassanein and Kharoob [16]. The moment-gradient factor C_b was found to influence by the girder geometry and slenderness for the case of HTFPGs with slender stiffened webs [17].On the other hand, an experimental and analytical research investigated the structural characteristics of lean duplex stainless steel I-sections by Saliba and Gardner [18]. Tadeh Zirakian [19], focused on LDB of doubly symmetric I-shaped members with slender web. Kalkan and Alper [20] studied the effect of web distortion in a lateral distortional buckling mode on the buckling moments of doubly symmetric steel IPGs analytically and numerically.

In 2018, Elkawas et al, studied LTB strength and behavior of high-strength steel corrugated web girders [21]. In 2019, Chen et al studied the mechanical properties and cross-sectional behavior of additively manufactured high-strength steel tubular sections [22].

In this research, LDB was studied on IPGs subjected to two type of loading. The aim of this study is getting $M_{cr,FE}$ and the value of C_b to the IPGs that have the buckling mode is LDB.

2. LDB OF CARBON STEEL IPGS

It was known also that the elastic LTB moment of IPGs under uniform bending was obtained from the following

equation [15],

$$M_{cr.o.LTB} = \frac{\pi}{kL}\sqrt{EI_y\, GJ\left(1+\frac{\pi^2}{(k_wL)^2}\frac{Ec_w}{GJ}\right)} \quad (1)$$

Where L is the unbraced length, k is the buckling coefficient regarding the out-of-plane flexural rotations at the supports, k_w is the buckling coefficient regarding the restrained warping at the supports, EI_y is the minor axis flexural rigidity, GJ is the torsional rigidity, and Ec_w is the warping rigidity. These are given by,

$$GJ = \frac{E}{6(1+\upsilon)}(2b_f{t_f}^3 + h_w{t_w}^3 \quad (2)$$

$$Ec_w = E\frac{t_f{b_f}^3(h_w+t_f)^2}{24} \quad (3)$$

where E is the Young's modulus, G is the shear modulus, υ is the Poisson's ratio, b_f is the flange width, t_f is flange thickness, h_w is the web height and t_w is the web thickness of the IPGs.

However, past research on carbon steel IPGs yielded a high level of understanding their LDB behavior. Accordingly, Pi and Trahair [23] showed that the elastic LDB moment ($M_{cr,o,LDB}$) might be obtained from (4). Their main idea suggests that a reduction in the warping stiffness due to web distortions should be taken into account in addition to a reduction in the torsional stiffness when calculating the LDB moment of an IPG with stocky flanges.

$$M_{cr.o.LDB} = \frac{\pi}{kL}\sqrt{EI_y\, GJ_e\left(1+\frac{\pi^2}{(k_wL)^2}\frac{Ec_{we}}{GJ_e}\right)} \quad (4)$$

$$GJ_e = \frac{(2GJ_f)(\frac{12D_WL^2}{\pi^2h_w})}{(2GJ_f)+(\frac{12D_WL^2}{\pi^2h_w})} \qquad with\ D_W = \frac{Et_w{}^3}{12(1-\upsilon^2)} \quad (5)$$

$$Ec_{we} = \frac{Ec_w}{1+rf_w{}^3(\frac{h_w}{12l_b})(1+\frac{b_f}{h_w})} \quad (6)$$

where GJ_f is the torsional rigidity of the flange and rf_w is the smaller of t_f/t_w and 2. The reduced torsional (GJ_e) and warping (Ec_{we}) rigidities, as given above, were shown to approach the torsional (GJ) and warping (Ec_w) rigidities as the flange stockiness and the web slenderness of IPG.

Current design codes [24, 25, 26] account for the influence of the moment gradient on the IPGs through a modification coefficient factor that is referred to as the moment gradient coefficient (C_b). This coefficient relates the critical buckling moment M_{cr} for a girder subjected to concentrated load to the corresponding critical buckling moment $M_{o,cr}$ of the same girder under a uniform end moment, as given by (7).

This coefficient relates the critical buckling moment M_{cr} for IPG subjected to specific transverse load to the corresponding critical buckling moment $M_{o,cr}$ of the same IPG under a uniform moment, as given by (7). The value of this non-dimensional factor is always greater than 1.0 for a varying bending moment diagram.

$$C_b = \frac{M_{cr}}{M_{o,cr}} \quad (7)$$

3. FINITE ELEMENT MODELLING

A. Current FE model

Using ABAQUS [14], 3-D FE models for simply supported IPGs subjected to two load cases (uniform end moment and mid-span concentrated load at shear center). The buckling modes are estimated through the Eigenvalue analysis. This is a linear analysis performed using the (*BUCKLE) procedure available in the ABAQUS library with the load applied within the step. The first buckling mode occurred in the eigenvalue analysis was used to estimate the FE critical bending moment ($M_{cr,FE}$). The following sections includes considerations in choosing the mesh, material modeling, and modeling of the boundary conditions, load application and verification of the model.

B. Element type, mesh and material properties

The four-node thin shell elements with reduced integration S4R was used in the current FE model, which is the same element used in the FE model of [15]. S4R has six degrees of freedom per node, provides high accuracy for most of thin-walled girder applications and allows for transverse deformation. The FE also accounts for finite strain and is suitable for large strain analysis. Simpson rule with five integration points was used through the included element thickness. As mentioned in [16], the researchers were found that a mesh size of 50 mm is appropriate for the purpose of this work. The young's modulus E_o = 200GPa, Poisson's ratio υ= 0.3 were considered.

C. Load application and boundary conditions

Two types of load application was applied on the FE model, as shown in Fig. 2. The first one was a uniform bending moment about the major axis of the IPGs over the unbraced lengths. To avoid any undesirable localized web deformations and stress on centration, the end moment loading was simulated with couple of forces in the form of uniform loading applied at the top and bottom flanges of the IPGs. In this loading type, the top flange is subjected to compressive longitudinal forces, while the bottom flange is subjected to tensile forces opposing the compressive ones. The second load application was a concentrated load at shear center of IPGs in mid-span. The boundary conditions are taken herein following the work conducted numerically in [27]. However, simply supported boundary conditions are applied to end sections. As shown in Fig. 2, at each end section, the twist rotation about z-axis of all nodes of the section is restrained ($\emptyset_z$= 0:0). The lateral displacement in x-axis of all nodes on the y-axis (at x = 0:0) is restrained (U_x= 0:0). The vertical displacement of the center of the web is restrained (U_y= 0:0), while the longitudinal displacement in z-axis of a center point at the lower flange is restrained (U_z= 0:0). It should be noted that current boundary conditions and load application provide the most conservative loading distribution.

D. Stiffeners arrangement

Using transverse stiffeners along the girder length influence the failure mode in the IPGs. In addition, Akay et al. [28] found that the lateral distortional buckling of IPGs may be enhanced by using transverse stiffeners to prevent distortion by coupling the rotational degree of freedom of the top and bottom flanges. White and Jung [29] found that when the limit on the maximum stiffener spacing of a/h_w=3 is satisfied throughout the unbraced length of IPGs, the web distortion effects will in general be reduced; where a is the web panel width of the IPGs [30]. This mean, using the previous stiffeners spacing leading to LTB mode.

4. Verification of FE model

A verification test has been carried out on the six models of IPGs with different dimensions, as given in Table (1). The maximum stiffener spacing of a/h_w <3.0 is considered to prevent the web distortional. Two types of load application was applied on the models as discussed previously. The girders were subjected to uniform bending moment about the major axis of the IPGs over the unbraced lengths. However, the same girders were subjected to concentrated load in mid-span at shear center. The critical bending moment due to uniform end moment ($M_{cr,FE}$) and the critical bending moment due to concentrated load ($M_{cr,FE,c}$) were calculated from FE models. Then, the values of $M_{cr,FE}$ were compared with the critical bending moment ($M_{o,cr}$) given by (1). The results showed that $M_{cr,FE}$ was in good agreement with $M_{o,cr}$ as shown in Table 2. It can be seen that the mean value and standard deviation of $M_{cr,FE}/M_{o,cr}$ are 0.99 and 0.005 respectively.

Moreover, the values of the bending coefficient factor (C_b) for models were calculated from (7) as shown in Table 2. The results showed that the average of C_b was 1.35 which is the same as recommended by [26].

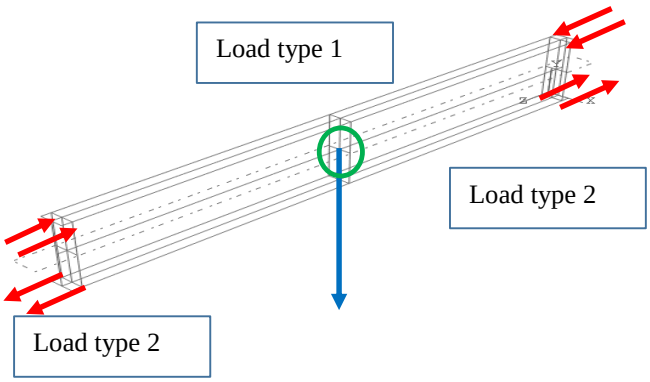

Figure 2. Load application and boundary conditions of the FE model

TABLE 1
GEOMETRICAL PROPERTIES OF IPGS.

Models	L [m]	b_f [mm]	t_f [mm]	t_w [mm]	h_w [mm]
1	9	250	30	10	1140
2	11	350	30	10	890
3	1	300	30	10	1000
4	15	300	30	10	1250
5	17	250	30	10	1140
6	19	250	30	10	1140

TABLE 2
$M_{cr,FE,c}$, $M_{cr,FE}$, $M_{o,cr}$ AND C_b VALUES.

Models	$M_{cr,FE,c}$ $[KN.m]$	$M_{cr,FE}$ $[KN.m]$	$M_{o,cr}$ $[KN.m]$	$M_{cr,FE}/M_{o,cr}$	C_b
1	1749.3	1336.4	1352.87	0.99	1.34
2	2724.8	2034.2	2008.05	1.01	1.34
3	1511.25	1122.4	1130.75	0.99	1.35
4	1365.8	1014.9	1025.15	0.99	1.35
5	712.9	526.5	536.19	0.98	1.35
6	614	453.9	465	0.98	1.35
			Average	0.99	1.35
			STDEV	0.01	0.01

5. Preliminary analysis

The main purpose of this research is to study the IPGs failed by LDB. So, a preliminary analysis was developed using ABAQUS program [14] to estimate the limits which LDB occurred. A series of elastic buckling analysis is carried out on 12 groups. The classification of the flanges in the IPGs in the current analysis were compact and non-compact flanges while the web plate was slender. The limits of compact and non-compact flanges in Euro code [25], are shown in the following equations.

$$c/t \leq 10\varepsilon \quad \text{for compact flanges} \tag{8}$$

Where: $t = t_f$

$$c = (b_f - t_w)/2 \tag{9}$$

And $\varepsilon = \sqrt{235/f_y}$ (10)

In addition, the limits of non-compact section for flange was:

$$c/t \leq 14\varepsilon. \quad \text{for non-compact flanges} \tag{11}$$

As can be seen in Fig. 3, h_w represent web depth, t_w denotes the web thickness, b_f (flange width) and t_f (flange thickness). There are two compact flanges and two non-compact flanges were used in the study. The thickness of compact flanges were 25mm and 30mm. Moreover, the thickness of non-compact flanges were 18mm and 20mm. The flange width (b_f) and the web height (h_w) of IPGs were constant which equal 250mm and 1000mm, respectively The web plate slenderness is characterized by web height to web thickness (h_w/t_w) values that assumes 166.667, 125 and 100 for web thickness 6, 8 and 10mm respectively. Each cross section was modeled with 8 different spans (4, 6, 8, 10, 12, 14, 16, 20m). Table 3, explained the dimension of sections (t_f and t_w) and flange classification where b_f and h_w are constant as mentioned previous.

Fig. 4 showed the relation between relative girder slenderness (λ) and critical bending moment according to uniform end moment ($M_{cr,FE}$) for all groups. Where$\lambda = L_b/r_y$, L_b is the laterally unbraced length and r_y is the radius of gyration of the compression flange where $r_y = \sqrt{I_y/A}$ According to [29] and [30], the purpose of using such

stiffeners in the IPGs was to prevent the occurrence of the local web crippling. Therefore, we should using stiffeners at supports and in mid-span and this leading to LDB mode. The aim of this study, getting the values of λ_1 and λ_2 as shown in fig. (4). When$\lambda \leq \lambda_1$, the buckling mode is LB, $\lambda_1 \leq \lambda \leq \lambda_2$, the buckling mode is LDB and $\lambda \geq \lambda_2$, the buckling mode is LTB. As shown in fig. 4, we noticed that, the minimum value of λ_1 which its buckling mode was LDB is 90 and the maximum value of λ_2 is 221. So, when λ between 90 and 221, the buckling mode was LDB. When$\lambda \leq 90$, the buckling mode was LB. When$\lambda \geq 221$, the buckling mode was LTB. The relative girder slenderness for LDB mode assumes 90 to 221 for unbraced length between 6m to14m respectively in this study.

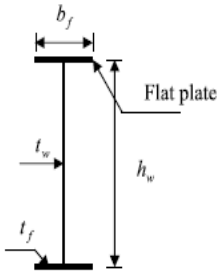

Figure 3. I-section plate girder.

TABLE 3.
THE DIMENSION OF DIFFERENT CROSS SECTION

Groups	t_f [mm]	t_w [mm]	Flange classification
G1	18	6	Non-compact
G2	18	8	Non-compact
G3	18	10	Non-compact
G4	20	6	Non-compact
G5	20	8	Non-compact
G6	20	10	Non-compact
G7	25	6	Compact
G8	25	8	Compact
G9	25	10	Compact
G10	30	6	Compact
G11	30	8	Compact
G12	30	10	Compact

6. PARAMETRIC STUDY

A parametric study was developed using ABAQUS program [14] to simulate the behavior of IPGs. The study performed using 72 IPGs where the girders divided into 36 non-compact IPGs sections and 36 compact IPGs sections. The parameters covered herein are based upon the EC3 [25] recommendations. Parametric studies for IPGs are carefully designed based on three parameters: the unbraced length (L), the web plate thickness (t_w) and the flange thickness (t_f). The parameters are included the unbraced length (L) which its buckling mode was LDB assumes five values (6, 8, 10, 12, 14m) according to preliminary analysis.

7. RESULTS

Table 5 and Table 6 show the results of the parametric study. It is clear that from Table 5 and 6, the value of $M_{cr,FE}$ was smaller than value of $M_{cr,FE,c}$ due to the uniform end moment loading case is worst loading case. Consequently, It is necessary account for the influence of the moment gradient on the IPGs through a modification coefficient factor that is referred to as the moment gradient coefficient (C_b) as in (7). Fig. 5-a and Fig. 5-b demonstrates the variation of the C_b coefficient against the length of girders for the simply supported IPGs subjected to mid-span concentrated loads.

As can be seen, Fig. 5-a represent non-compact section, whereas t_f =20mm and Fig. 5-b represent compact section, whereas t_f =25mm. This trend shows that the length of girders values assumes (6, 8m, 10m, 12m, 14m) and the C_b coefficient has its maximum value for longer spans that are characterized by lower lengths. A reduction in the C_b value is demonstrate for IPGs having shorter spans. With the increase in unbraced length and thickness of web, its C_b value is close to 1.35 and the type of failure mode is LTB as shown in Fig. 5-a and Fig. 5-b. This case can be noticed that for length 14m at (t_w=10m).

It can be observed that the path of the moment coefficient factor-unbraced length are nearly linear and coincident as the IPGs have lengths (8m to 14m). As it can be seen from Fig. 5 -a and Fig. 5-b, these girders fail by LDB. In shorter lengths, the girders fail by LB with decreasing in the web plate thickness as length 6m at t_w=6mm. It is clear that the variation of flange thickness (t_f) does not significantly affect that C_b value from 6m to 14m as evident in Fig. 5-a,b and Table 4. Table 6 explained at length 6m are affected by the flange thickness increasing as it decreases.

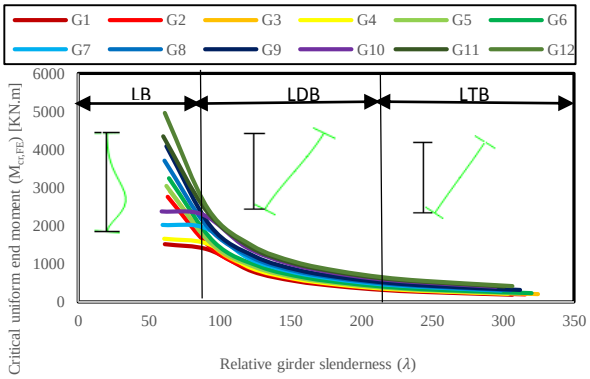

Figure 4. The relation between relative girder slenderness and $M_{cr,FE}$ for all groups.

(a)

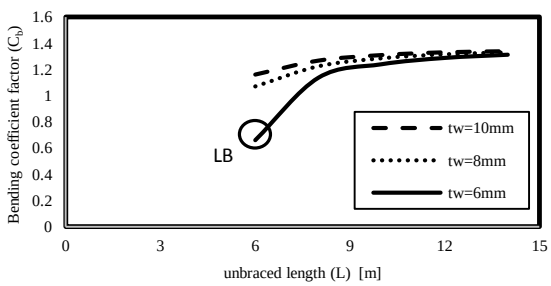

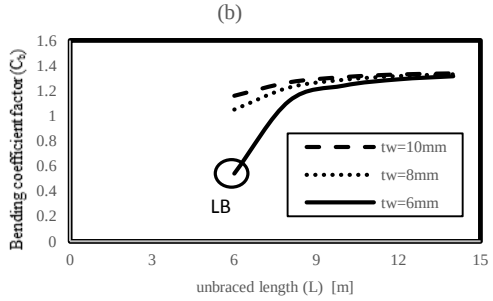

Figure 5. The effect of unbraced length and on C_b; (a) t_f=20mm, (b) t_f=25mm.

As explained earlier, Table (4) explained the values of the bending coefficient factor (C_b) to specimens, which had h_w/t_w=125. It is clear that from Table (4), the C_b values for length (6, 8, 10, 12, 14m) were constant by changing the thickness of flange in lengths from 8m to 14m and this means, the increasing in flange thickness does not effect on C_b values with a clear effect.

TABLE 4
C_b VALUES FOR SPECIMENS, WHICH HAD h_w/t_w=125

Section type	L(m) / t_f(mm)	6	8	10	12	14
Non compact	18	1.07	1.22	1.28	1.32	1.33
	20	1.07	1.22	1.28	1.32	1.33
Compact	25	1.06	1.22	1.29	1.32	1.33
	30	1.01	1.22	1.29	1.32	1.33

8. MODE OF FAILURE

As a result of the preliminary analysis, the failure mode for most specimens which have lengths from 6m to 14m were LDB. Except few of these specimens failed LB and LTB as shown in table (5) and (6). Fig. 6 explain the relation between the web plate slenderness ratio (h_w/t_w) and bending moment coefficient factor (C_b). As shown in Fig. 6, the path of lengths (10, 12, 14m) is linear. These girders fail by LDB. At lengths (6, 8m), the value of ($C_b < 1$) and this is refer to the buckling mode is LB. this case occurs in shorter lengths and when the web plate slenderness ratio increases as obvious in Fig. 6.

8.1 EFFECT OF LENGTH

A. Non-compact section

The effect of the unbraced length could be examined by the analysis of the IPGs with non-compact flanges as shown in Table 5. The thickness of flange in these girders was maintained, which equal 18mm. While, the main variable in these girders was the unbraced length, which assumes 6m, 8m, 10m, 12m, and 14m. The web plate slenderness assumes 166.667, 125 and 100 for web thickness 6, 8 and 10mm respectively. However, the results indicated that increasing the length of girders decreases $M_{cr.FE}$ and $M_{cr.FE,c}$ as shown in Fig. 7-a which represent the relation between unbraced length in horizontal axis and $M_{cr.FE}$ in vertical axis and Fig. 7-b which represent the relation between unbraced length and $M_{cr.FE,c}$. As shown in Fig. 7-a and Fig. 7-b explained the decrease in (h_w/t_w) leads to increase in $M_{cr.FE}$ and $M_{cr.FE,c}$ with small value. As shown in Fig. 7-a, In three cases of web thickness, the path of the moment-unbraced length curves are coincident that's where most of the girders fail by LDB. For Fig. 7-b, the paths of three curves are nearly coincident except at a length of 6m where it is buckling mode was LB.

B. Compact section

By analysis of compact girders which had flange thickness equal 30mm as shown in Table 6, where the length only was variable. It's found that, the $M_{cr.FE}$ and $M_{cr.FE,c}$ values increased due to increase in thickness of flange. Also, the increasing in length leading to decreasing in both $M_{cr.FE}$ and $M_{cr.FE,c}$ with the same amount of shortfall on the previous girders as shown in Fig. 8-a and Fig. 8-b respectively. From Fig. 8-a, all curves take the same path and be close to each other where it is buckling mode is LDB. Fig. 8-b, the path of girders have 6m and 8m was differ from rest of girders due to its buckling mode was LB. As previously mentioned, with decreasing in the unbraced length and the web thickness and increasing in the flange thickness leads to LB mode.

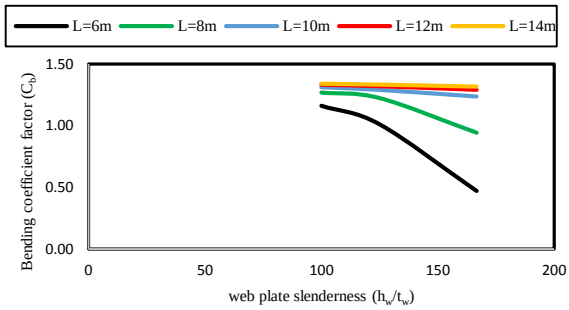

Figure 6. Values of C_b for girders that flange thickness 30mm.

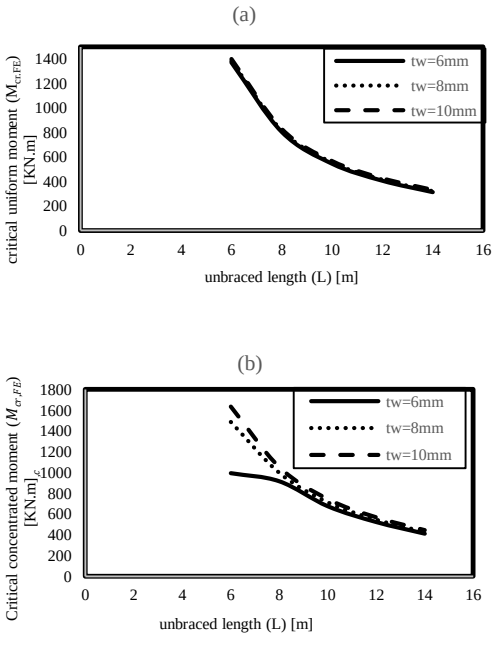

Figure 7. Effect of the unbraced length on$M_{cr,FE}$ and $M_{cr,FE,c}$.

TABLE 5
THE GEOMETRY OF NON-COMPACT SECTION.

Specimens	t_f [mm]	t_w [mm]	$[h_w/t_w]$	L [m]	$M_{cr,FE,c}$ $[KN.m]$	$M_{cr,FE}$ $[KN.m]$	C_b	Buckling mode
1	18	6	166.67	6	993.87	1371.51	0.72	LB
2	18	6	166.67	8	915.94	805.08	1.14	LDB
3	18	6	166.67	10	675.5	545.88	1.24	LDB
4	18	6	166.67	12	523.47	407.16	1.29	LDB
5	18	6	166.67	14	411.53	314.07	1.31	LDB
6	18	8	125	6	1487.85	1385.28	1.07	LDB
7	18	8	125	8	997.86	815.76	1.22	LDB
8	18	8	125	10	713.025	555.03	1.28	LDB
9	18	8	125	12	546.12	415.2	1.32	LDB
10	18	8	125	14	427	321.21	1.33	LDB
11	18	10	100	6	1634.4	1402.47	1.17	LDB
12	18	10	100	8	1051.48	829.65	1.27	LDB
13	18	10	100	10	742.85	567.15	1.31	LDB
14	18	10	100	12	567	426.06	1.33	LDB
15	18	10	100	14	443.24	331.08	1.34	LTB
16	20	6	166.67	6	1016.13	1531.98	0.66	LB
17	20	6	166.67	8	1025.84	903.15	1.14	LDB
18	20	6	166.67	10	762.7	615.69	1.24	LDB
19	20	6	166.67	12	594.3	461.79	1.29	LDB
20	20	6	166.67	14	469.945	358.38	1.31	LDB
21	20	8	125	6	1655.85	1546.2	1.07	LDB
22	20	8	125	8	1119.4	914.7	1.22	LDB
23	20	8	125	10	803.95	625.74	1.28	LDB
24	20	8	125	12	618.96	470.61	1.32	LDB
25	20	8	125	14	486.71	366.15	1.33	LDB
26	20	10	100	6	1821	1564.14	1.16	LDB
27	20	10	100	8	1177	929.34	1.27	LDB
28	20	10	100	10	835.625	638.37	1.31	LDB
29	20	10	100	12	640.86	481.8	1.33	LDB
30	20	10	100	14	503.51	376.17	1.34	LTB

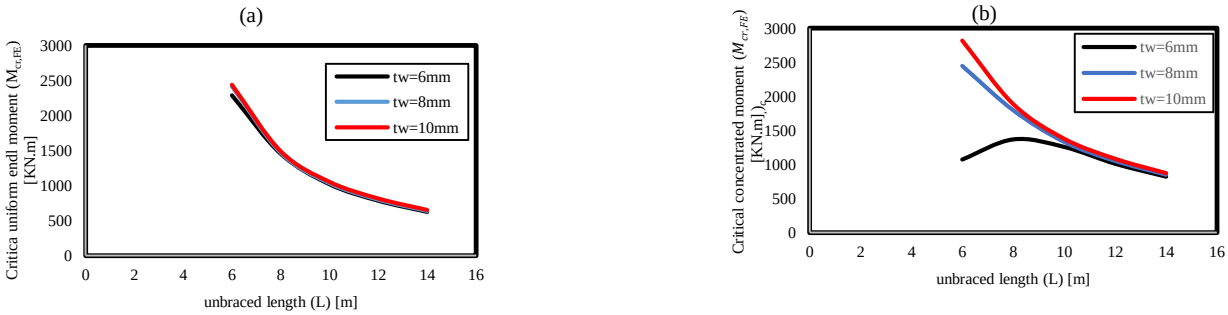

Figure 8. Effect of the unbraced length on (a) $M_{cr,FE}$and (b) $M_{cr,FE,c}$

Table (6)
THE GEOMETRY OF COMPACT SECTIONS

Specimens	t_f [mm]	t_w [mm]	$[h_w/t_w]$	L [m]	$M_{cr,FE,c}$ $[KN.m]$	$M_{cr,FE}$ $[KN.m]$	C_b	Failure mode
31	25	6	166.67	6	1052.1	1943.61	0.54	LB
32	25	6	166.67	8	1301.2	1164.66	1.12	LDB
33	25	6	166.67	10	997.9	805.11	1.24	LDB
34	25	6	166.67	12	789.6	612.06	1.29	LDB
35	25	6	166.67	14	633.5	481.95	1.31	LDB
36	25	8	125	6	2072.7	1966.05	1.05	LDB
37	25	8	125	8	1443.68	1178.31	1.23	LDB
38	25	8	125	10	1052.375	817.74	1.29	LDB
39	25	8	125	12	820.98	623.49	1.32	LDB
40	25	8	125	14	654.465	491.97	1.33	LDB
41	25	10	100	6	2308.2	1985.85	1.16	LDB
42	25	10	100	8	1514.48	1195.32	1.27	LDB
43	25	10	100	10	1089.65	832.44	1.31	LDB
44	25	10	100	12	846.21	636.27	1.33	LDB
45	25	10	100	14	673.365	503.07	1.34	LTB
46	30	6	166.67	6	1073.16	2285.25	0.47	LB
47	30	6	166.67	8	1367.5	1452.03	0.94	LB
48	30	6	166.67	10	1257.075	1017.54	1.24	LDB
49	30	6	166.67	12	1011	782.91	1.29	LDB
50	30	6	166.67	14	822.115	624.03	1.32	LDB
51	30	8	125	6	2446.5	2414.22	1.01	LDB
52	30	8	125	8	1795.46	1467.3	1.22	LDB
53	30	8	125	10	1331.15	1032.75	1.29	LDB
54	30	8	125	12	1051.92	797.4	1.32	LDB
55	30	8	125	14	849.065	637.2	1.33	LDB
56	30	10	100	6	2818.8	2435.49	1.16	LDB
57	30	10	100	8	1886.08	1486.92	1.27	LDB
58	30	10	100	10	1376.4	1050.27	1.31	LDB
59	30	10	100	12	1081.89	812.76	1.33	LDB
60	30	10	100	14	871.115	650.43	1.34	LTB

8.2 EFFECT OF WEB PLATE SLENDERNESS (h_w/t_w)

A. Non-compact sections

The effect of web plate slenderness (h_w/t_w) is discussed herein; see Fig. 9-a. Herein, as well, it is obvious that decreasing in the slenderness of web plate (h_w/t_w) and the other dimensions are kept constant, where the section dimension was (b_f =250mm, t_f =18mm and h_w =1000mm) leads to increase of $M_{cr,FE}$ with small value. Figure 9-b also shows an increase of length along with decrease in web plate slenderness ratio affected the value of ($M_{cr,FE,c}$) by relatively little increase. It is obvious from Fig. 9-b, due to decrease in h_w/t_w, there was an small increase in $M_{cr,FE,c}$ values for all lengths except at 6m length. The rate of increase is significant as a result of the mode of buckling was LB.

B. 10.2 Compact sections

Fig. 10-a explains the relationship between $M_{cr,FE}$ and the web plate slenderness ratio. The web plate slenderness was variable and the other dimensions are constant. The section used is compact, whereas (b_f =250mm, t_f =25mm and h_w =1000mm). From Fig. 10-a and Fig. 10-b It is clear that increasing in (h_w/t_w) lead to decrease in both of $M_{cr,FE}$ and $M_{cr,FE,c}$ by a small percentage and increasing in the unbraced length also leads to decrease in $M_{cr,FE}$ and $M_{cr,FE,c}$. From Fig. 10-a and Fig. 10-b. It is clear that, the inclination of the lengths

are the same. Except for the length of 6m, there is a difference in tendency from the rest of the lengths as shown in Fig. 10-a. This can be explained by the difference in buckling mode was LB as shown in Table 6. It is obvious that from Fig. 9 and Fig. 10, decreasing in the flange thickness t_f leading to decrease in $M_{cr,FE}$ and $M_{cr,FE,c}$.

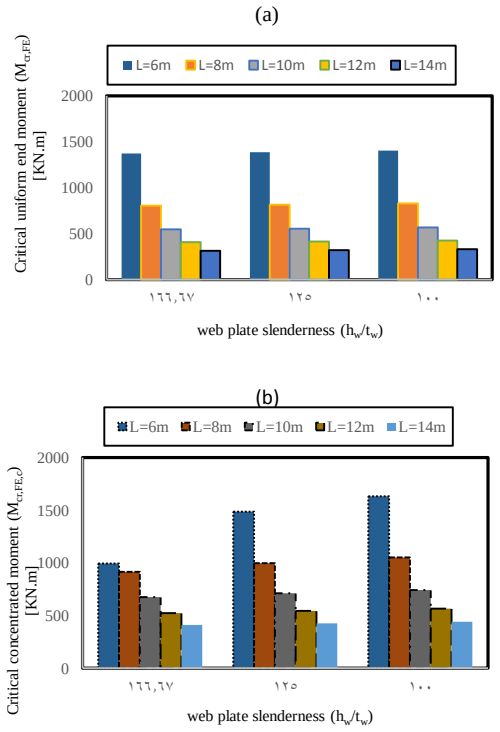

Figure 9. Effect of web plate slenderness; (a) $M_{cr,FE}$and (b) $M_{cr,FE,c}$.

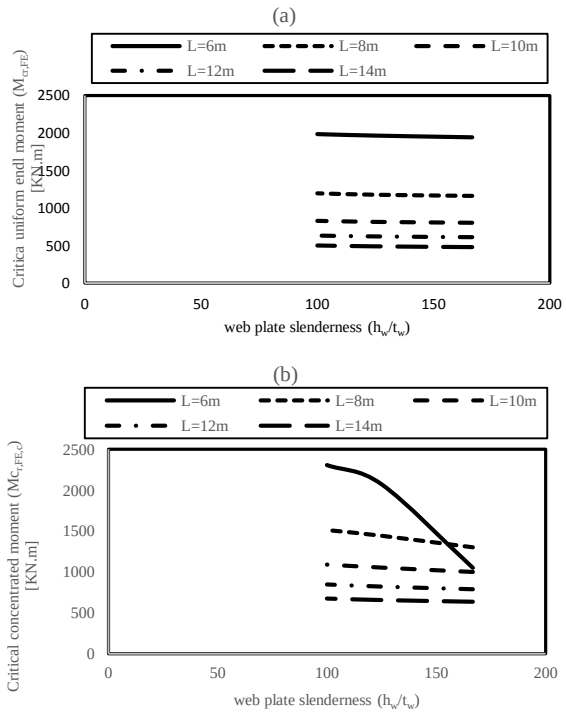

Figure 10. Effect of web plate slenderness on; (a) $M_{cr,FE}$and (b) $M_{cr,FE,c}$.

8.3 Effect of flange thickness (t_f)

Fig. 11 explained the relationship between flange thickness on horizontal axis and $M_{cr,FE}$ on vertical axis, whereas flange thickness was variable and rest of parameters were constant. It is clear that the increase in t_f leads to increasing in $M_{cr,FE}$ and $M_{cr,FE,c}$ values for h_w/t_w=166.67, 125, and 100 as shown in Fig. 11 and 12 respectively. These figures also explained the increasing in length of girders leads to decrease in $M_{cr,FE}$ and $M_{cr,FE,c}$ as previously mentioned in the effect of unbraced length paragraph. From Fig. 11 and Fig. 12, The paths of curves have almost the same inclination because the girders have the same buckling mode as LDB. Except Fig. 12-a, at 30mm flange thickness, 6mm web thickness and (6, 8m) unbraced length, failure mode was LB. As a result type of buckling mode, the curve of (6, 8m) unbraced length was different on the rest of other lengths.

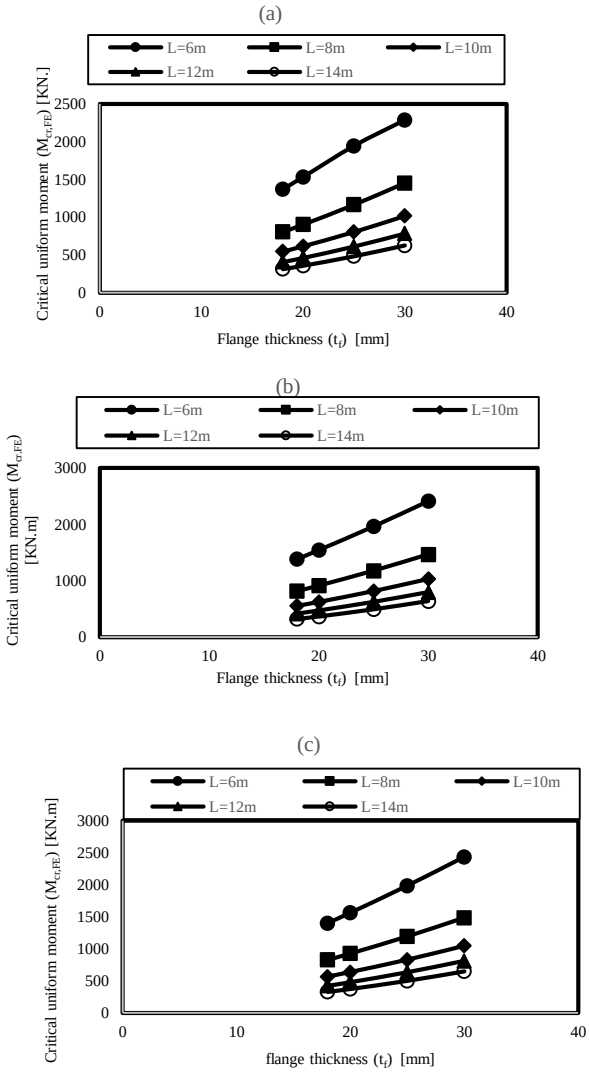

Figure 11. Effect of flange thickness on$M_{cr,FE}$; (a) h_w/t_w=166.67, (b) h_w/t_w=125, (c) h_w/t_w=100.

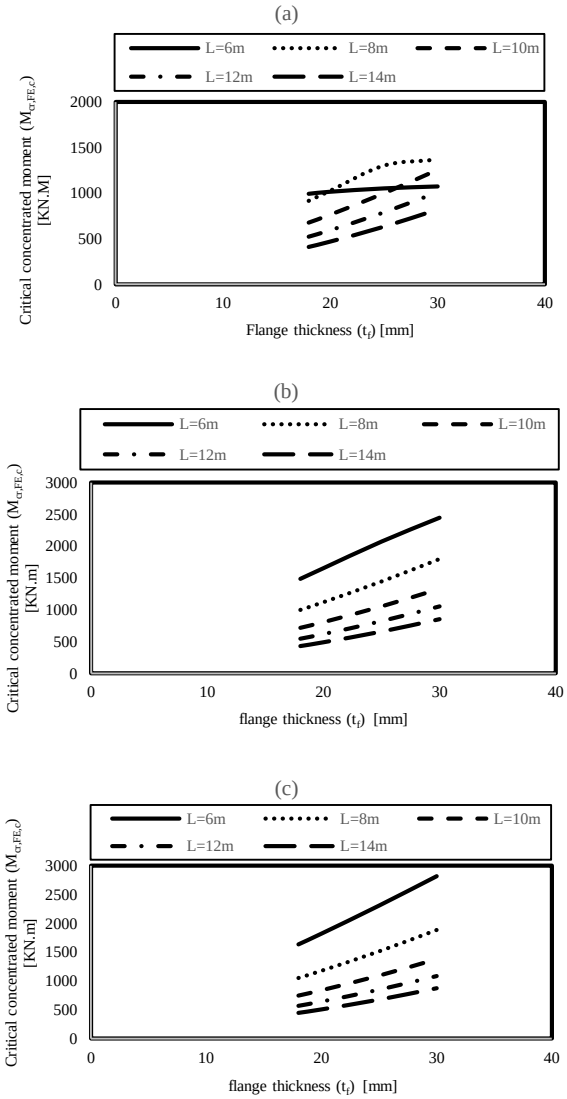

Figure 12. Effect of flange thickness on$M_{cr,FE,c}$; (a) h_w/t_w=166.67, (b) h_w/t_w=125, (c) h_w/t_w=100.

8.5 THE C_b COEFFICIENT FOR LATERAL DISTORTIONAL BUCKLING OF IPGS

The previous results indicate that the C_b coefficient of IPGs, which had LDB mode, may have a different value from C_b value of LTB which equal 1.35.Table 7 explained C_b and λ values for specimens which failure mode of it is LDB.

From Table 8, the limits of λ ranges from 90 to 221 as previously mentioned. Due to the accuracy of the C_b value of LDB, for this it was necessary to divide λ into three parts. Table 8 explained λ ranges and C_b values of its ranges.

From Table 8, it is clear that the average and standard deviation value of λ limits (90:124) iare1.13 and 0.06 respectively. For λ limits (125:175), the mean value and standard deviation of C_b are 1.27 and 0.03 respectively. As for λ limits (176:221), the mean value and standard deviation of C_b are 1.32 and 0.02 respectively.

TABLE 8

LIMITS OF λ AND ITS CORRESPONDING C_b VALUES.

	Limits of λ		
	90 to 124	125 to 175	176 to 221
values of C_b that corresponding to λ values	1.14	1.24	1.29
	1.07	1.28	1.31
	1.22	1.31	1.32
	1.17	1.24	1.33
	1.14	1.28	1.33
	1.07	1.31	1.29
	1.16	1.24	1.31
	1.12	1.29	1.32
	1.05	1.31	1.33
	1.23	1.24	1.33
	1.16	1.29	1.29
	1.01	1.27	1.31
	1.16	1.27	1.32
	-	1.27	1.33
	-	1.22	1.33
	-	1.27	1.29
	-	1.22	1.32
	-	-	1.32
	-	-	1.33
	-	-	1.31
	-	-	1.33
Average	1.13	1.27	1.32
STDEV	0.06	0.03	0.02

9. CONCLUSIONS

The linear elastic lateral–distortional buckling of IPGs under moment gradient was studied by means of the finite element method. The main aim was to investigate the effects of unbraced length, web plate slenderness and the flange thickness on the C_b, $M_{cr,FE}$, $M_{cr,FE,c}$ and buckling modes. It was found that the C_b factors increase with increasing in unbraced length, web thickness and the flange thickness. The same is for $M_{cr,FE}$, $M_{cr,FE,c}$ except in the case of increasing the unbraced length the both of $M_{cr,FE}$ and $M_{cr,FE,c}$ decrease. As for the buckling mode, we notice that the increase in unbraced length, web thickness and flange thickness leading to LTB mode. In medium unbraced lengths, the buckling mode is LDB. In few cases such as decreasing in web thickness and flange thickness, the buckling mode is LB. As a result of parametric study, the mean value and standard deviation of C_b for LDB mode are 1.13 and 0.06 respectively for λ limits (90:124). For λ limits (125:175), the mean value and standard deviation of C_b are 1.27 and 0.03 respectively. As for λ limits (176:221), the mean value and standard deviation of C_b are 1.32 and 0.02 respectively.

TABLE (7)

VALUES OF C_b FOR SPECIMENS WHICH BUCKLING MODE OF IT IS LDB

Groups	Specimens No.	C_b	λ	Groups	Specimens No.	C_b	λ
Group 1	2	1.14	122.55	Group 7	32	1.12	119.39
	3	1.24	153.19		33	1.24	149.24
	4	1.29	183.83		34	1.29	179.08
	5	1.31	214.46		35	1.31	208.93
Group 2	6	1.07	94.66	Group 8	36	1.05	91.58
	7	1.22	126.21		37	1.23	122.10
	8	1.28	157.76		38	1.29	152.63
	9	1.32	189.31		39	1.32	183.16
	10	1.33	220.87		40	1.33	213.68
Group 3	11	1.17	97.32	Group 9	41	1.16	93.57
	12	1.27	129.76		42	1.27	124.76
	13	1.31	162.21		43	1.31	155.95
	14	1.33	194.65		44	1.33	187.14
Group 4	17	1.14	121.43	Group 10	48	1.24	147.51
	18	1.24	151.79		49	1.29	177.01
	19	1.29	182.15		50	1.32	206.52
	20	1.31	212.50	Group 11	51	1.01	90.23
Group 5	21	1.07	93.57		52	1.22	120.30
	22	1.22	124.76		53	1.29	150.38
	23	1.28	155.95		54	1.32	180.45
	24	1.32	187.14		55	1.33	210.53
	25	1.33	218.33	Group 12	56	1.16	122.55
Group 6	26	1.16	96.00		57	1.27	153.19
	27	1.27	128.00		58	1.31	183.83
	28	1.31	160.00		59	1.33	214.46
	29	1.33	192.00				

REFERENCES

[1] Hancock GJ, Bradford MA, Trahair NS. "Web distortion and flexural–torsional buckling". J Struct Div ASCE 1980;106(ST7):1557–71.

[2] Bradford MA, Trahair NS. "Distortional buckling of I-beams". J Struct DivASCE 1981;107(ST2):355–70.

[3] Roberts TM, Jhita PS. "Lateral, local and distortional buckling of I-beams". Thin-WalledStruct 1983;1:289–308.

[4] Bradford MA. "Distortional buckling of monosymmetric I-section beams".J Construct Steel Res 1985;5:123–36.

[5] Bradford MA. "Inelastic distortional buckling of I-beams". Comput Struct 1986;24:923–33.

[6] Bradford MA. "Lateral–distortional buckling of Tee-section beams". Thin Walled Struct 1990;10:13–30.

[7] Bradford MA. "Lateral–distortional buckling of I-section members".J Construct Steel Res 1992;23:97–116.

[8] Hughes O, Ma M. "Lateral–distortional buckling of monosymmetricbeams under point load". J Struct Mech ASCE 1996;122(10):1022–9.

[9] Ma M, Hughes O. "Lateral–distortional buckling of monosymmetric Ibeams under distributed vertical load". Thin Walled Struct 1996;26(2):123–45.

[10] Avik samanta, Ashwini kumar. "Distortional buckling in monosymmetric I-beams" Thin-walled structures 44 (2006) 51-56

[11] Tadeh Zirakian. "Elastic distortional buckling of doubly symmetric I-shapedflexural members with slender webs" Thin-Walled Structures 46 (2008) 466–475.

[12] Ilker Kalkan, Alper Buyukkaragoz. "A numerical and analytical study on distortional buckling of doubly-symmetric steel I-beams" Journal of Constructional Steel Research 70 (2012) 289–297.

[13] Song, Yuan. "Combined web distortional and lateral-torsional buckling of partially restrained I-section beams" International journal of mechanical sciences131-132 (2017) 107-112.

[14] ABAQUS Standard User's Manual, Hibbitt, Karlsson and Sorensen, Inc, Vol. 1, 2 and 3, Version 6.6, USA, 2007.

[15] M.F. Hassanein, N. Silvestre. "Flexural behavior of lean duplex stainless steel girders with slender unstiffened webs" J Struct Eng 85 (2013) 12-23.

[16] M.F. Hassanein, O.F .Kharoob. "Flexural strength of hollow tubular flange plate girders with slender stiffened webs under mid-span concentrated loads" Thin-Walled Structures 69(2013)18–28.

[17] M.F. Hassanein n, O.F. Kharoob and A.M. ElHadidy "Lateral–torsional buckling of hollow tubular flange plate girders with slender stiffened webs". Thin-Walled Structures 65 (2013) 49–61.

[18] N. Saliba, L. Gardner "Cross section stability of lean duplex stainless steel welded I-sections". Journal of constructional steel research 80(2013) 1-14.

[19] Tadeh Zirakian, "Elastic distortional buckling of doubly symmetric I-shaped flexural members with slender webs", Thin-walled structures 46 (2008) 466-475.

[20] Ilker Kalkan, Alper, " A numerical and analytical study on distortional buckling of doubly-symmetric steel I-beams", Journal of Constructional Steel Research, 70 (2012) 289-297.

[21] AA Alkawas, MF Hassanein, M Elchalakani. "Lateral- torsional buckling strength and behavior of high-strength steel corrugated web girders for bridge construction", Thin-walled structures 62 (2018) 578-587

[22] JJ Yan, MT Chen, WM Quach, M Yan, B Young "Mechanical properties and cross-sectional behavior of additively manufactured high-strength steel tubular sections", Thin-walled structures 72 (2019) 354-573.

[23] Pi YL, Trahair NS. "Distortion and warping at beam supports". ASCE J Struct Eng2000;126:1279–87.

[24] AISC, "Load and resistance factor design specification, for structural steel buildings". Chicago: American Institute of Steel Construction; 1999.

[25] Euro code3, "Design of steel structures" – part 1.1: general rules and rules for buildings, ENV 1993-1-1, CEN; 2004.

[26] AISC, "Load and Resistance Factor Design Specification, for Structural Steel Buildings". Chicago: American Institute of Steel Construction; 2010

[27] Dong J, Sause R. "Flexural strength of tubular flange girders". Journal of Constructional Steel Research 2009; 65: 622–30.

[28] Akay HV, Johnson CP, Will KM. "Lateral and local buckling of beams and frames". Journal of the Structural Division, ASCE 1977; 103(3):1821–32.

[29] White DW, Jung S. "Effect of web distortion on the buckling strength of non-composite discretely braced steel I-section members". Engineering Structures 2007; 29:1872–88.

[30] Nguyen CT, Moon J, Le VN, Lee H. "Lateral–torsional buckling of I-girders with discrete torsional bracings". Journal of Constructional Steel Research 2010;66:170–7.